Send Orders for Reprints to reprints@benthamscience.net

1 *Current Microwave Chemistry,* XXXX, *XX,* 1-15

RESEARCH ARTICLE

Microwave Thermal Treatment for the Recovery of Re in Copper and Molybdenum Concentrates

Vanesa Bazan[1,*], Ariel Maratta[1], Gastón Villafañe[1], Pablo Pacheco[2] and Elena Brandaleze[3]

[1]CONICET, Institute of Mining Research, Universidad Nacional de San Juan, Av. Libertador General San Martin 1109, Oeste, San Juan, Argentina; [2]INQUISAL, Centro Científico-Tecnológico de San Luis [CCT-San Luis], CONICET-Universidad Nacional de San Luis, Chacabuco y Pedernera, San Luis, 5700, Argentina; [3]Department of Metallurgy & Center DEYTEMA, Facultad Regional San Nicolás, Universidad Tecnológica Nacional, Colón, 332- [B2900LWH] San Nicolás, Argentina

ARTICLE HISTORY

Received: November 22, 2023
Revised: February 29, 2024
Accepted: March 01, 2024

DOI:
10.2174/0122133356290503240509092306

Abstract: ***Background*:** Rhenium [Re] is obtained as a by-product during the extraction of copper and molybdenum ores. In current extractive metallurgy, Re extraction involves a heat treatment that causes Re losses by volatilization and release of toxic gases into the environment.

***Objective*:** This research proposes a novel microwave heat treatment [MWHT] to enhance Re extraction avoiding Re losses and toxic gas release into the environment.

***Method*:** A novel MWHT and traditional thermal processes used in mining were applied to Cu-Mo concentrates. The elemental composition analysis of the concentrate was performed by atomic spectrometry. The crystalline phase was identified by X-ray diffraction. Particle structure observations were performed with an optical microscopy [OM] and scanning electron microscopy [SEM] with a Field Emission, including semiquantitative analysis [EDS]. Thermal behavior and non-isothermal reduction processes were studied using Thermogravimetry Differential Thermal Analysis [TG-DTA].

***Result*:** Re, S and As release decreased 5% during MWHT, compared to 34% of traditional methods. Molybdenite [MoS_2] and Chalcopyrite [$CuFeS_2$] were the crystalline phases in the ore after MWHT. Rhenium was found as an oxide [ReO_3] and metallic Re. Samples under MWHT showed structural transformations in the mineral particles, with minimal mass losses and high Re and Mo concentrations. The structural transformation of the ore involved microcracks formation.

***Conclusion*:** The MWHT induces a combination of particle degradation mechanisms and lower temperature requirements that prevent Re losses. Lower gas emissions turn this technology into an environmentally friendly one. Crystalline transformation of the Re-chalcopyrite phase enhances Re release during leaching, the next step after MWHT in the hydrometallurgical extraction.

Keywords: Copper ores, molybdenum ores, microwaves, microwave heat treatment, rhenium.

1. INTRODUCTION

Re constitutes a valuable and extremely rare chemical element, currently used in numerous applications: a] in metallurgy as an addition element [for high-temperature superalloys], b] as a catalyst in the petrochemical industry, c] in electronic equipment, and d] in medicine for pancreatic cancer therapy [1-7]. Minerals containing Re are generally found in very small quantities and are currently not commercially viable sources. Re is present in nature at low concentrations as an isomorphic impurity in more than 50 carrier minerals such as molybdenite [MoS_2] and chalcopyrite [$CuFeS_2$]. In both cases, it is associated with complex sulphide minerals [8-11]. Rhenium has different industrial methods for production [12-15]. The most used is molybdenite roasting. The mechanism is associated with molybdenum production. First, flue gases [SO_2] are released from the ore by oxidative roasting. This is possible since Re volatilizes at temperatures above 400°C in the form of rhenium heptaoxide [Re_2O_7]. The ore is then treated by leaching and solvent extraction to obtain Re [16-20]. This method has advantages, such as large capacity, easy operation, and low demand for equipment. It also has significant shortcomings. During the oxidation-roasting process, dust with harmful gases are emitted [MoS_2, MoO_3, MoO_2, SO_3, SO_2], and certain amounts of Re_2O_7 can be lost [17, 21, 22]. These ga emissions constitute unacceptable air pollution and damage to the extractive metallurgy equipment, increasing production costs [17, 23, 24]. Mining's impact on climate change and gas emissions mitigation purposes is under the spotlight in scientific studies. M. Azadi *et al.* [25] inform that emissions from coal mining are well studied and are expected to reach approximately 784 Mt of CO_2-equivalent [CO_2e] by

*Address correspondence to this author at the CONICET, Institute of Mining Research, Universidad Nacional de San Juan, Av. Libertador General San Martin 1109, Oeste, San Juan, Argentina; E-mail: bazan@unsj.edu.ar

2213-3356/24 $65.00+.00

2030. In this sense, it is relevant to extend research to extractive metallurgy processes, such as roasting heat treatments, in order to develop new alternatives to minimize gas emissions and improve energy consumption. Nowadays, rhenium is mainly produced through the molybdenum roasting and copper smelting processes. However, compared to the hydrometallurgical process, the pyrometallurgical process consumes more energy and discharges larger amounts of waste gas, requiring expensive gas treatment or causing serious environmental problems [20, 26]. In addition, due to its recovery as a by-product from the gas phase in smelting and roasting, the total recovery of rhenium in those processes is of key importance.

Furthermore, to overcome the shortcomings of oxidative roasting during Re extraction, a microwave heat treatment [MWHT] has been introduced as a roasting alternative [27-29]. MW is associated with electromagnetic radiation in the microwave frequency range of 300 MHz - 300 GHz. Some researchers carried out experimental exploration and theoretical analysis of microwave irradiation's influence on mineral microstructure [30-33]. MW heating of a refractory mineral is more efficient compared to conventional roasting processes, resulting in lower energy costs. Refractory mineral compounds have different absorption properties in the MW field, causing temperature gradients within the particles that promote microcracks generation. The temperature gradients produce localized "hot spots" that result in areas with high temperatures that induce phase transformations in the structure and localized volume changes. Studies have been conducted on the effect of content on MW-induced cracking [34-38]. It was demonstrated that MW radiation has a significant impact on the pore structure when the coal body's moisture content is low, and this behavior can be assimilated to sulphide minerals due to its oxygen affinity. MW heating is more efficient than conventional heating in terms of speed and uniformity [17, 39-41]. It is important to consider that MW heating occurs from the core of the particles as the MW penetrates and generates heat inside the sample. On the opposite, in conventional heating processes, particles are heated from the surface to the core by conduction or convection. The reverse MW heating pattern is considered extremely useful for mineral treatment processes when the heat has to be trapped inside the material [39, 42, 43]. In addition, MW contributes to the propagation of microcracks due to electromagnetic vibrations. Numerous experiments and numerical research have been carried out into the mechanism governing the MW-induced fracturing of rocks [or ores] and the influence of MWHT on the mechanical properties of rocks [or ores] [44-47]. Under the effect of MWHT, new intergranular and transgranular fractures are generated in rocks [48-51]. More seriously, rocks are cracked and crushed or molten to cause rocks [or ores] to lose all of their bearing capacity. The mineral particles cracks, and the rupture improves Re recovery during leaching and solvent extraction, decreasing energy requirements during milling processes. Although the use of microwaves is not at an industrial scale in the roasting stage of pyrometallurgical routes, in recent years, many studies have been devoted to this pretreatment technique [52-54]. Accordingly, emerging applications of microwave-assisted roasting [MWAR] to treat sulfide materials such as gold concentrates and mixed oxide-sulfide zinc ores have recently been reported. In the present work, a methodology for Re extraction from copper and molybdenum ores employing MWHT is proposed. To evaluate the performance of the proposed methodology, a comparative study between MWHT, oxidative roasting and carbothermal reduction was carried out. The characterization of the treated mineral samples includes the chemical composition determination and the crystalline phases identification by X ray diffraction [XRD]. In order to identify gas emissions, chemical reactions, and phase transformations in relation to temperature, differential thermal analysis tests [DTA TG] were performed at a constant heating rate [β = 10 ºC min^{-1}]. The structure and the presence of microcracks in the particles were evaluated by optical microscopy and scanning electron microscopy [SEM with EDS analysis]. The results were correlated with the information of the thermodynamic simulation of the systems, considering specific conditions of interest.

2. MATERIALS AND METHODS

In this study, microwave irradiation treatment was carried out in a 2.45 GHz multimode furnace [model JQ280IX] with a turntable and a maximum power of 1900 W. The chamber dimension was 333 x 548 x 525 mm. Samples of 10 g were placed in a porcelain crucible of 50 mL. The heat treatment power conditions selected were: 500 W, 750 W and 950 W. The samples were treated using periods of 10 min up to a total time of 30 min. Between heat periods, the temperature was measured with an infrared thermometer gun. Finally, samples were cooled and stored properly. Temperature variations in the sample during heat treatments were monitored with a GIS 1000C Professional Bosch thermal detector [-40°C to 1000°C].

For comparison, a sample of the concentrate was subjected to the carbothermal reduction process, and the working procedure and parameters were described in a previous study [55]. As was mentioned, the capture values and the reducing agent were adjusted in order to retain the highest sulfur concentrations. The temperature and time conditions were established to reach the highest recovery of the desired elements. To remove impurities, the Re-containing molybdenum-copper sulphide concentrates were treated by an alkaline leaching process. The leaching agent was a sodium hydrosulphide solution in the presence of sodium hydroxide NaSH/NaOH. For the comparative study, the sample with the highest Re content was selected.

The study also included a sample processed by conventional roasting heat treatment, processed in air at 400°C for 30 min. All the samples and heat treatment conditions are detailed in Table **1**.

Table 1. Samples identification and heat treatment conditions used in the study.

Sample	Heat Treatments Conditions
S1	Conventional roasting - processed at 400°C for 30 min.
T1	Carbothermal roasting with CaO [0.2 g] and C [0.5 g], heated to 400°C for 30 min.
MW	MW [500 W, 750 W and 950 W], considering periods of 10 min and t_{total} = 30 min

The chemical composition of the samples S1, T1, and MW was determined by different atomic spectroscopy techniques according to the concentration of the target element. The samples [0.2 g to 0.5 g] were digested by applying a multi-acid media depending on the analytical technique. A double attack sequence was performed. Finally, samples were diluted to 5% [v v^{-1}] nitric acid. Major elements were determined by atomic absorption spectroscopy in Perkin Elmer equipment, AA PinAAcle 900T. The minor elements were determined by inductively coupled plasma optical emission spectrometry [ICP-OES] instrument PERKIN ELMER 7300 DV. The sample MW heat treated applying 750W showed the highest Re content and was selected for further studies.

The crystalline phase identification was carried out by X-ray diffraction using a Philips X 'Pert diffractometer and the software Match 3.0 for data processing.

The structure of the concentrate particles was observed by optical microscopy [OM] using an Olympus GX51 microscope with a Material Plus image analysis system and a Zeiss microscope with polarized light and differential interference contrast microscopy [DIC]. The structural study also included the observation carried out by scanning electron microscopy [SEM], including semi-quantitative analysis [EDS], with a Field Emission Gun, FEI QUANTA 200. The thermal behavior of the samples, including the non-isothermal reduction process, was determined by thermal analysis [DTA TG] using a SHIMADZU TA 60 instrument. Tests were performed up to 700ºC, considering a heating rate of 10ºC min^{-1} in air. The results are correlated with the thermodynamic simulation carried out by FactSage 8.1 [56]. The databases used were: FTmisc 8.1, FTOxCN 8.1, FToxid 8.1, FTsalt 8.1, FactPS 8.1.

3. EXPERIMENTAL

Sample preparation: for the Rhenium recovery study, a copper, iron, and molybdenum sulphide mineral from a deposit placed in the central zone of Argentina was selected. The mineral was processed by "rougher" flotation. Then, samples were crushed and pulverized [up to 100 mesh granulometry] in order to improve Re extraction. Once the samples reached the appropriate size, they were homogenized and hermetically preserved in polypropylene containers. Roasting stage: from the processed sample, 10 g were weighed and placed in a 50 mL porcelain crucible. It was exposed to MW radiation in 3 periods of 10 minutes of 500, 750, and 950 W [30 min]. Finally, the sample was cooled and stored. Re extraction methodologies involved an initial characterization of the molybdenite sample without heat treatment. Then, the proposed treatment was applied to the mineral, along with two other commonly used techniques, in order to evaluate and compare the efficiency of the different processes. In summary, the treatments were:

• Sample S1: processed at 400°C for 30 min.

• Sample T1: processed [by carbothermal roasting] with CaO [0.2 g] and C [0.5 g], heated to 400°C for 30 min.

• Sample MW: processed with MWHT for 30 minutes [technique proposed in this work]. Subsequently, tests were carried out on the processed samples in order to characterize them and compare the results.

4. RESULTS AND DISCUSSION

For comparison, the ores treated by the described roasting treatments were characterized according to their chemical composition, crystalline phases, and morphology. The chemical composition of the samples is shown in Table **2**. The sample identified as S0 shows the chemical composition of the molybdenite [MoS_2] concentrate without heat treatment. For validation of the spectroscopic methodology performed for Re determination, a standard reference material was analyzed [423-Molybdenum Oxide Concentrate, with a certified rhenium concentration of 0.004%]. The average Re concentration value obtained for the reference material was 0.0038%, with no significant difference [p= 0.05] with the certified Re concentration value.

Table 2. Chemical composition of the samples in wt %.

Sample	S_0	S_1	T_1	MW
Cu	2.5±3	1.92±3	1.37±3	1.15±3
Fe	2.7±3	1.07±3	1.91±3	2.37±3
Na	0.18±3	0.06±3	0.06±3	0.12±3
K	0.15±3	0.11±3	0.11±3	0.13±3
Mo	49.48±3	50.67±3	55.10±3	56.77±3
Mn	0.01±3	0.01±3	0.01±3	0.01±3
Ca	0.57±3	0.50±3	5.92±3	0.61±3
Mg	0.20±3	0.18±3	0.17±3	0.22±3
Re	0.65±3	0.43±3	0.63±3	0.62±3
S	29.89±3	23.05±3	25.53±3	27.18±3
As	0.20±3	0.05±3	0.05±3	0.18±3

It is relevant to note that sample T1 and sample MW presented the highest Re concentrations [0.63 %wt.] and [0.62 %wt.], respectively. These results are consistent with those reported by Juneja *et al*. [23]. Although Re recoveries are similar in carbothermal and MWHT, the recoveries of S and As after MWHT are close to the concentration of S and As in the mineral without thermal treatment. The values indicate that no harmful emissions of SO_2 and AsO_3 were generated during MWHT.

The crystalline phases present in the samples after heat treatments were identified by XRD, as shown in Fig. **1**. The results showed that the main crystalline phases determined in all the samples are Molybdenite [MoS_2] and Chalcopyrite [$CuFeS_2$]. Rhenium is present in all the samples as oxide [ReO_3] and metallic Re. In sample T1, carbide [$CFeORe_2$] was also identified. The information obtained is consistent with the chemical composition of the samples.

XRD results also provided information on the crystalline structure present in the identified phases. The main phase [MoS_2] was a hexagonal crystalline structure after the proposed heat treatments. The tetragonal crystalline structure of chalcopyrite constitutes the most common phase in nature. However, the $CuFeS_2$ [chalcopyrite] phase presents a crystalline structure transformation between tetragonal and cubic

phase FCC compatible with the intermediate solid solution cubanite [57]. These data allow us to infer how MWHT favors the generation of microcracks with the exposure temperature, retaining the rhenium in the calcine as an oxide.

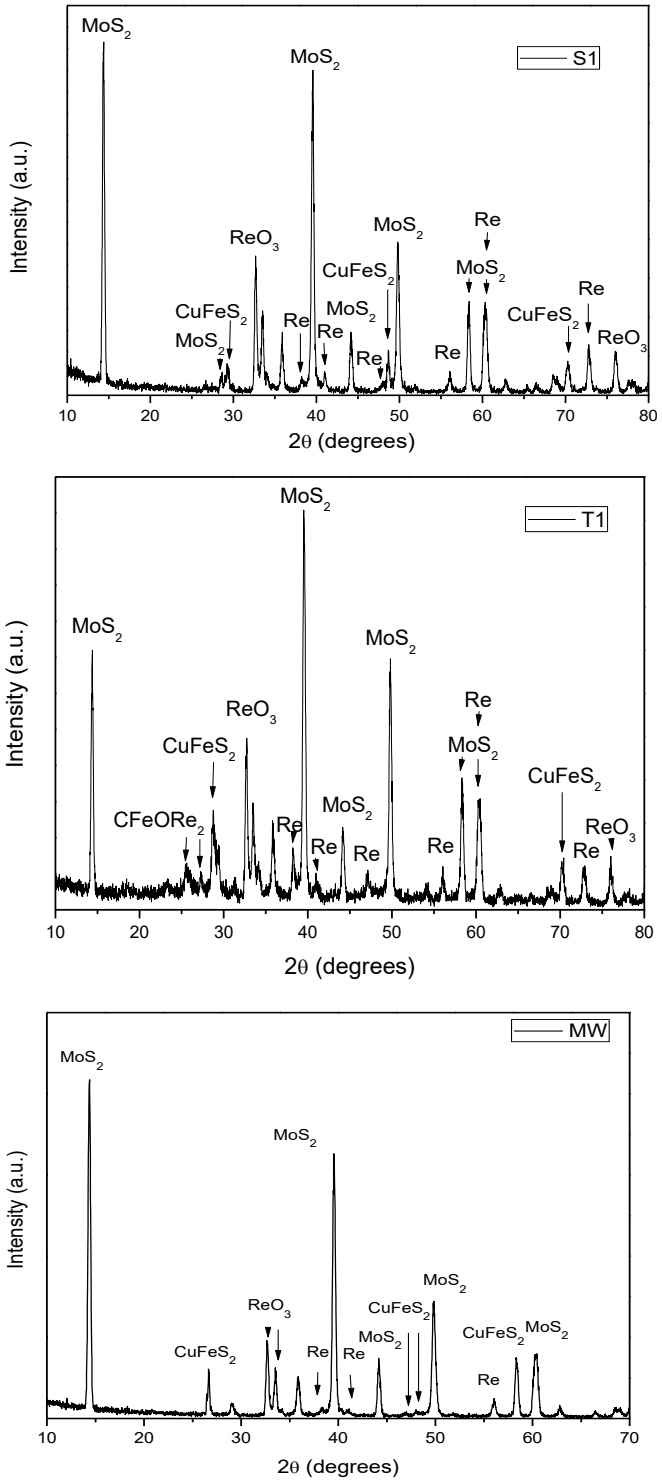

Fig. [1]. Crystalline phases identified in samples. [a] S1, [b] T1 and [c] MW.

The reactivity of the sulfides or transformation to metal sulfides and the reactions associated with metal sulfides in an oxidizing atmosphere [such as roasting treatments] may be established by thermodynamic calculations. In the samples, it is possible to propose the following reactions [eq. 1 to 4] to explain the products identified by XRD diffraction. The enthalpy evolution [ΔH0 and ΔG0, in cal] in relation to temperature [T, in °C] for all reactions was calculated by applying the Reaction module of the software FactSage 8.1. The range of temperature considered in the thermodynamic simulation was 100°C to 800°C, with a temperature of 50°C. In addition, it was possible to evaluate Gibbs energy variations ΔG0 at T=400°C, verifying that all of them were negatives. The feasibility of the reactions at 400ºC could be proposed in the order: ΔG30 > ΔG10> ΔG20> ΔG30.

$ReS_2 + 2\ O_2 \rightarrow Re + 2\ SO_2$ [1] ΔG10400ºC= -108417.4cal

$Re + 1.5\ O_2 \rightarrow ReO_3$ [2] ΔG20400ºC= -97140.1cal

$MoS_2 + 3\ O_2 \rightarrow MoO_2 + 2SO_2$ [3] ΔG30400ºC= -194292.3cal

$2\ MoO_2 + O_2 \rightarrow 2\ MoO3$ [4] ΔG40400ºC= -52653.1cal

Plotting ΔG0 at temperatures between 100 to 800°C makes it possible to compare the evolution predicted for all the reactions (Fig. **2**). Based on the thermodynamic prediction, the reaction (eq. 3) of MoS_2 roasting is probable at a temperature range of 100ºC to 800ºC. The corresponding reactions (eq. 1 and eq. 2) also are possible at the same temperature conditions. However, at T= 251ºC, both lines present a crossing point. At higher temperatures, the ReS_2 reaction with oxygen to form metallic Re (eq. 1) is more probable and predominant. This means that metallic Re is accumulated in the system at temperatures higher than 251ºC since it is probable at higher temperatures. Nevertheless, part of the metallic Re could be transformed in ReO_3 because eq. 2 also presents a negative value of ΔG0 up to 800ºC. The formation of MoO_3 (eq. 4) is also feasible according to the negative value of ΔG0 but with the lowest prevalence.

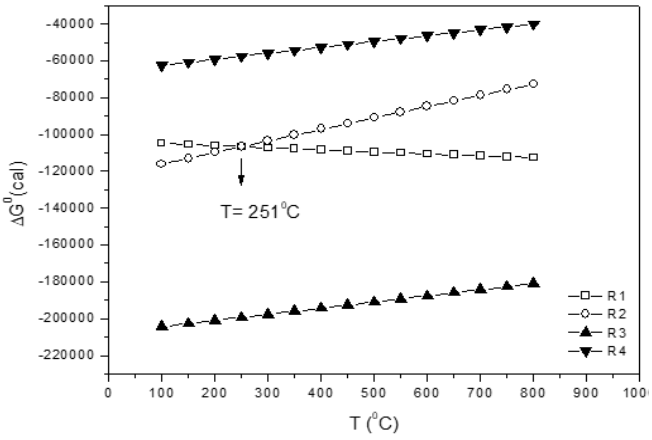

Fig. [2]. ΔG0 evolution at temperatures between 100 to 800°C of the eq.1 to 4.

The experimental results obtained through differential thermal analysis tests provided experimental relevant information on the thermal behavior of the samples. For this reason, the correlation between theoretical predictions and experimental results is considered necessary to provide a complete evaluation of the system.

The thermal behavior of the MW sample was determined by DTA TG tests up to 750ºC (Fig. **3**). The DTA curve shows the main exothermic peak at TpMW = 535°C. The DTA curve of this sample also presents slope changes at T1= 570°C, T2= 595°C and T3= 667°C compatible with structural transformations in the mineral particles since no changes of mass were registered in the TG curve at the mentioned temperatures.

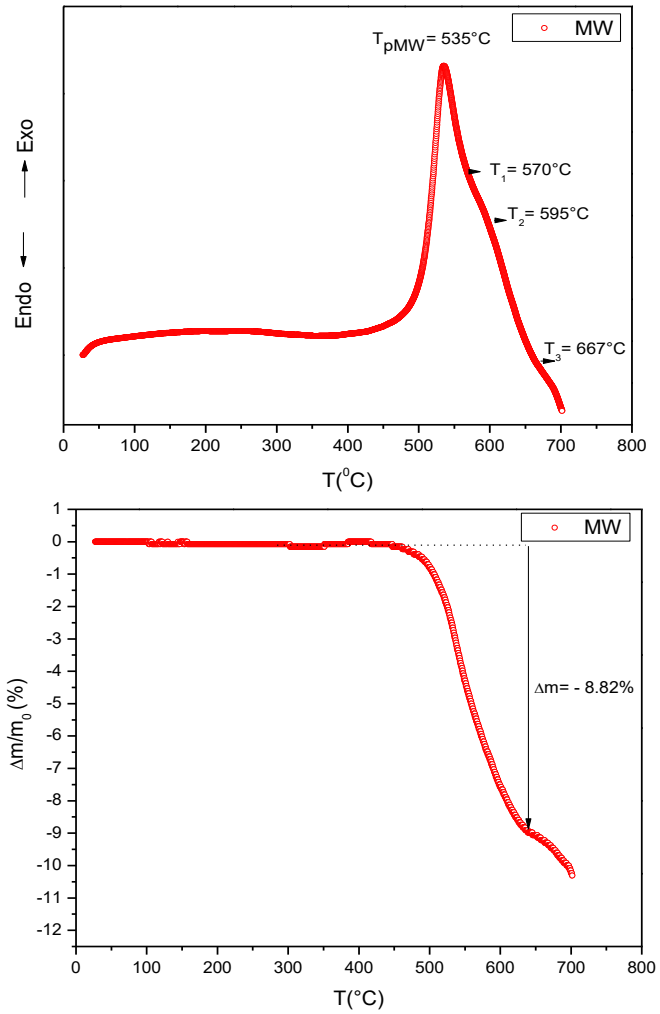

Fig. (3). Thermal behaviour of the sample MW. [a] DTA curve and [b] TG curve. (*A higher resolution/colour version of this figure is available in the electronic copy of the article*).

Fig. **4** shows the thermal behaviour of S1 and T1 samples obtained under the same conditions as the MW sample. DTA curves of samples S1 and T1 showed exothermic peaks at: TpS1 = 555°C and TpT1 = 505°C, Fig. **4** (a). The MW sample presented an intermediate value at TpMW = 535°C. The comparison between the three DTA curves showed that samples T1 and MW presented slope changes in a similar temperature range (between 565°C to 595°C), not clearly visualized for sample S1. In addition, it is observed that the exothermic peaks determined in the three samples present different values caused by the differences in the heating process conditions. This affirmation is consistent with others reported [55]. The exothermic reaction is attributed and justified by a mechanism involving molecular oxygen diffusion from the air into the molybdenite (MoS_2) particles. The oxygen reacts with MoS_2 to gradually form the following products: MoO_2 at 400ºC (eq. 3), MoO_3 at 555ºC (eq. 4) and sulfates, explaining the mass increase (ΔmT1= +1.8%), determined for sample T1 at T 600°C. The information is consistent with other reported results [58, 59]. Wang *et al*. [60] described the reaction (eq. 3) as the most violent exothermic reaction, producing more than 85% of the total heat released. According to Kar [61], molybdenite oxidation reactions (ec. 3) and (ec. 4) are affected by the oxygen concentration in the atmosphere and the surface atomic force of the particles.

According to Horikoshi and Serpone [62], MWHT accelerates chemical reactions in comparison with other conventional heating methods under identical temperature conditions.

MWHT produced lower gas emissions and minor environmental impact. The MW reaction presented a mass loss of Δm=-8.82%, as observed in the TG curve, Fig. (**3b**), compared to T1, -10%, and S1, -18% (Fig. **4b**).

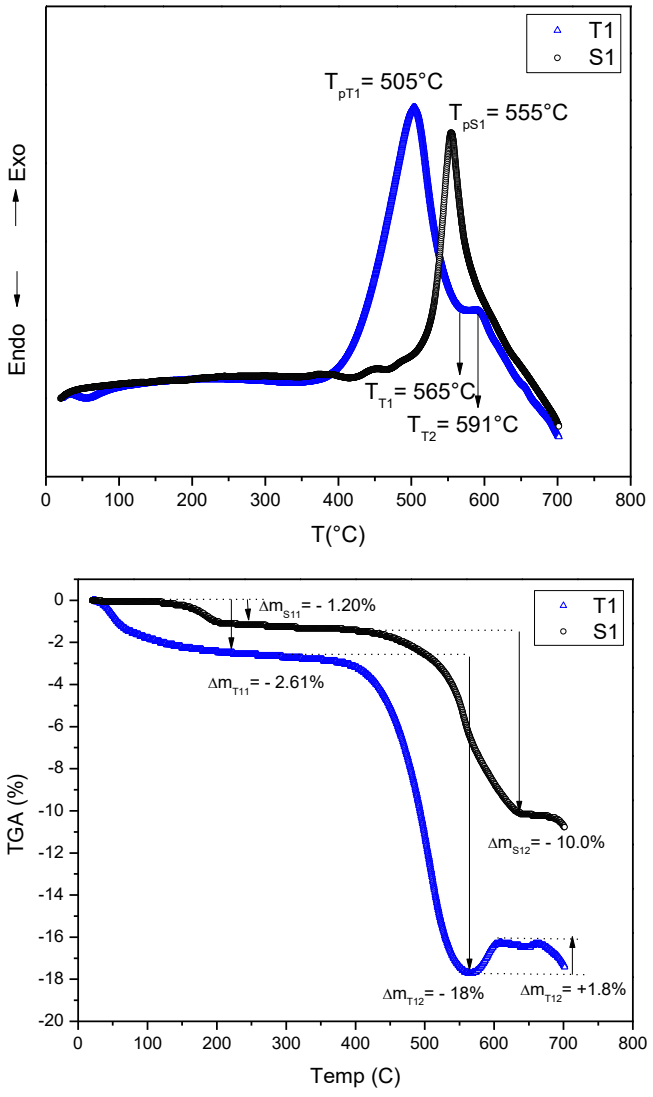

Fig. (4). Thermal behaviour of the samples S1 and T1. [a] DTA curves and [b] TG curves. (*A higher resolution/colour version of this figure is available in the electronic copy of the article*).

A structural study was carried out to corroborate the obtained results and to identify the MW mechanisms. This study involved optical microscopy [OM] and scanning electron microscopy [SEM-EDS analysis]. The presence of Molybdenite [MoS_2] and Chalcopyrite [$CuFeS_2$] particles was corroborated in all samples. Particles showed irregular morphologies and are constituted by different phases. In sample T1, carbon particles were observed. Both phases are commonly associated with other minerals and trace elements. In addition, by SEM and EDS analysis, the chemical composition of all the phases was determined. Metallic Re was detected inside the particles of molybdenite [MoS_2] and chalcopyrite [$CuFeS_2$]. These results agree with Drábek *et al*. observations [63]. Fig. (**5a-d**) shows the maps of the main elements: Mo, Cu, Fe and Re. Re is associated with the $CuFeS_2$ phase of the particle.

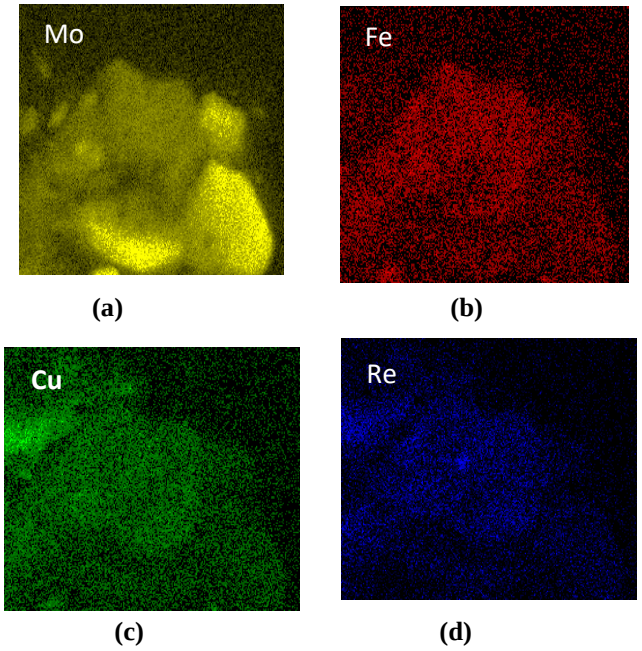

Fig. (5). Particle with Molybdenite [MoS_2] and Chalcopyrite $CuFeS_2$ that contain metallic Re. The information is corroborated by the maps of the elements (**a**) Mo, (**b**) Fe, (**c**) Cu and (**d**) Re, obtained by EDS. (*A higher resolution/colour version of this figure is available in the electronic copy of the article*).

The structural aspects determined through microscopy techniques corroborated the presence of different sulfide phases within the concentrate particles, as well as previous MW heat treatment. Fig. (**6a**) shows the aspect of the observed particles by SEM in the sample without heat treatment. In this case, the sample contains particles with irregular morphology and different colors according to the different mineral phases present. Through punctual EDS analysis, it was possible to establish that white phases are compatible with Chalcopyrite [$CuFeS_2$] associated with the other two phases: light gray and dark gray. The dark gray phase is mainly constituted by Si, Al, Ca, and Mg. In addition, isolated bright particles were also observed. The multi-component phases present in the mineral promoted the formation of localized heat point during MW treatment. MW treated particles are shown in Figure 6 [b]. A considerable change of the particles structural characteristics is visualized after the heat treatment at 750 W. The important quantity of identified fines showed considerable interface decohesion and particle fragmentation. The combination of degradation mechanisms such as microcracks, decohesion, and stratification is consistent with results reported by Horikoshi *et al*. [62] and Lu *et al*. [38]. Fig. (**6c**) shows in detail the internal fragmentation of the Chalcopyrite particles [white phase] produced by MW heat treatment, accelerating allotropic transformation. The produced micro-cracks improved the permeability and diffusion of the leaching solution into ore particles, improving metal recovery. In Fig. (**6d**), different phases [white spherical, irregular dark gray, and light polygonal gray phases] were identified within particles, probably as reaction products generated during the MW treatment.

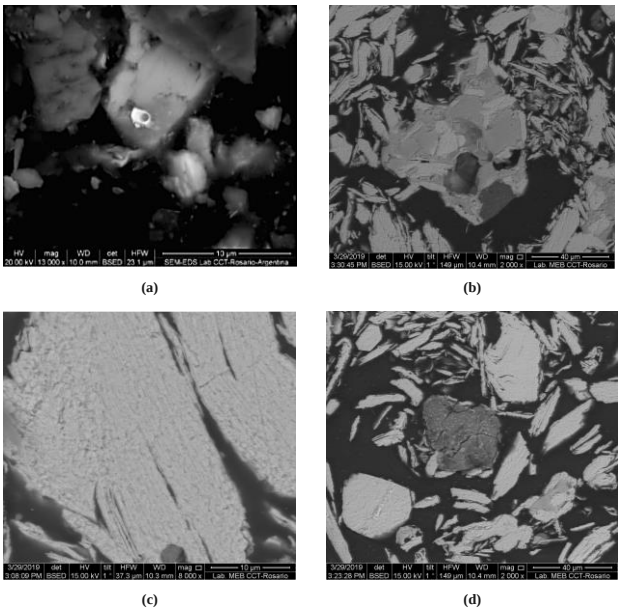

Fig. (6). Structural aspects determined through microscopy techniques. (**a**) Aspect of the mineral particles observed without heat treatment. (**b**) Aspect of the mineral particles observed with heat treatment S1. (**c**) Decohesion, fragmentation and microcracks observed in the MW mineral particles sample. (**d**) Different phases [white spherical, irregular dark gray and light polygonal gray phases] identified within part of the grey particles. (*A higher resolution/colour version of this figure is available in the electronic copy of the article*).

The degradation mechanisms verified by SEM on the MW sample are consistent with an allotropic crystalline phase transformation of the chalcopyrite [cubic to tetragonal]. This transformation involved volume changes and localized temperature differences caused by heat points produced by MW. The formation of microcracks in the mineral particles, including molybdenite, promoted a higher Re recovery during leaching in hydrometallurgy processes [64]. In addition, transversal cracks were also observed, consistent with particle degradation and thermal stress induced by thermal expansion. The thermal expansion after microwave irradiation is higher than the strength of the mineral particles [65-68]. The thermodynamic simulations carried out by FactSage 8.1 corroborated the lowest gas emissions produced for the MW. The emission is constituted mainly by SO_2. For the carbothermal roasting applied to the T1 sample, the emissions are constituted mainly by SO_2 and CO_2.

The solid phases predicted in samples S1, T1, and MW at each heat treatment condition confirm the generation of MoS_2, MoO_2, and ReS_2. Particularly in the MW sample, the predictions are consistent with a higher recovery of Mo and Re, determined by the chemical composition and X-ray diffraction. The increase of Mo content is justified by the presence of this element in five solid phases.

The increase of Mo concentration in the molybdenum concentrate is explained by considering gases released, mainly SO_2, decreasing the total mass of the concentrate (Eq. 1 and 2). Mo retention in the concentrate is also favored by MW radiation, increasing temperature up to 600°C, decomposing and oxidating MoO_3, Fe_3O_4 y WO_3. When temperature reaches 700°C, stable Mo complexes like $Fe_2[MoO_4]$ are formed [64].

MWHT applied on sulfide minerals could be considered as an ecofriendly alternative considering lower reaction times [even involving no solvent and no catalysts] and low gas emissions. The heating process by MW does not depend on heat conduction, for this reason, it is faster than conventional processes, and the heating efficiency is only influenced by the mineral particle composition. In addition, heating a solid by microwave radiation frequently generates hot spots [with 100 to 200 K above the temperature of the rest of the mass] as a result of differential heating. Accordingly, MW treatment can be useful in extractive metallurgy for refractory minerals, increasing internal cracking in ore particles and reaching higher metal recovery [46, 65, 69, 70].

CONCLUSION

The MW heat treatment induces a combination of particle degradation mechanisms that promote Re recovery, preventing losses during heat treatment. In addition, lower gas emissions combined with lower exothermic reactions produced by the MW heat treatment turns this type of technology into an environmentally friendly one. Thermal studies showed a lower temperature requirement during the MW heat treatment, which prevented Re losses by volatilization. This affirmation was confirmed by lower mass losses in the mineral samples. Thermodynamic simulation corroborates that the MW thermal treatment presents the lowest gas emissions, especially for SO_2. The MW heat treatment produces decohesion, generates microcracks by localized heating in the particles, and a crystalline structure transforms the chalcopyrite phase associated with molybdenite from cubic to tetragonal. The mentioned transformation produced volume variations that induced the nucleation and propagation of microcracks, causing fragmentation. Since Re is associated with chalcopyrite, this transformation could enhance future Re release during leaching, the next step after thermal treatment in hydrometallurgical extraction. The information obtained is applicable to extractive metallurgy processes of copper and molybdenum sulfide concentrates in order to achieve relevant economic benefits and minimal environmental impact.

CONSENT FOR PUBLICATION

Not applicable.

AVAILABILITY OF DATA AND MATERIALS

The data and supportive information are available within the article.

FUNDING

This work was financially supported by Agencia Nacional de Promoción Científica y Tecnológica [ANPCyT], grant number PICT-2019-00936.

CONFLICT OF INTEREST

The authors declare no conflict of interest, financial or otherwise.

ACKNOWLEDGEMENTS

Declared none.

REFERENCES

[1] McNulty, BA; Jowitt, SM Barriers to and uncertainties in understanding and quantifying global critical mineral and element supply. *IScience,* **2021**, *24*(7) http://dx.doi.org/10.1016/j.isci.2021.102809

[2] John, D.A. *Rhenium: a rare metal critical in modern transportation*; US Geological Survey, **2015**, pp. 2327-6932. http://dx.doi.org/10.3133/fs20143101

[3] Werner, T.T.; Mudd, G.M.; Jowitt, S.M.; Huston, D. Rhenium mineral resources: A global assessment. *Resour. Policy,* **2023**, *82*, 103441. http://dx.doi.org/10.1016/j.resourpol.2023.103441

[4] Lee, J.D.; Park, K.K.; Lee, M-G.; Kim, E-H.; Rhim, K.J.; Lee, J.T.; Yoo, H.S.; Kim, Y.M.; Park, K.B.; Kim, J.R. Radionuclide therapy of skin cancers and Bowen's disease using a specially designed skin patch. *J. Nucl. Med.,* **1997**, *38*(5), 697-702. PMID: 9170430

[5] Diksha, ; Kaur, M.; Megha, ; Reenu, ; Kaur, H.; Yempally, V. Rhenium (I) tricarbonyl complex with thiosemicarbazone ligand derived from Indole-2-carboxaldehyde: Synthesis, crystal structure, computational investigations, antimicrobial activity, and molecular docking studies. *J. Mol. Struct.,* **2024**, *1301*, 137319. http://dx.doi.org/10.1016/j.molstruc.2023.137319

[6] Hu, J.; Liu, Y.; Zhou, Y.; Zhao, H.; Xu, Z.; Li, H. Recent advances in rhenium-based nanostructures for enhanced electrocatalysis. *Appl. Catal. A Gen.,* **2023**, *663*, 119304. http://dx.doi.org/10.1016/j.apcata.2023.119304

[7] Pyczak, F.; Neumeier, S.; Göken, M. Temperature dependence of element partitioning in rhenium and ruthenium bearing nickel-base superalloys. *Mater. Sci. Eng. A,* **2010**, *527*(29-30), 7939-7943. http://dx.doi.org/10.1016/j.msea.2010.08.091

[8] Yan, L.; Fan, Y.; Huang, J.; Li, Y.; Zhou, T.; Zuo, T.; Zhang, Y.; Xu, G. Occurrence state and enrichment mechanism of rhenium in molybdenite from Merlin Deposit, Australia. *Ore Geol. Rev.,* **2023**, *162*, 105693. http://dx.doi.org/10.1016/j.oregeorev.2023.105693

[9] Zhao, H.; Huang, F.; Zhong, S.; Li, C.; Feng, C.; Hu, Z. The Wuliping ion-adsorption deposit, Guizhou Province, South China: A new type of rhenium (Re) deposit. *Ore Geol. Rev.,* **2023**, *160*, 105615. http://dx.doi.org/10.1016/j.oregeorev.2023.105615

[10] Schulz, K.J. *Critical mineral resources of the United States: economic and environmental geology and prospects for future supply,* 1st; Geological Survey, **2017**. http://dx.doi.org/10.3133/pp1802

[11] Barra, F.; Deditius, A.; Reich, M.; Kilburn, M.R.; Guagliardo, P.; Roberts, M.P. Dissecting the Re-Os molybdenite geochronometer. *Sci. Rep.,* **2017**, *7*(1), 16054. http://dx.doi.org/10.1038/s41598-017-16380-8 PMID: 29167505

[12] Bazan, V.; Brandaleze, E.; Santini, L.; Sarquis, P. Argentinean copper concentrates: structural aspects and thermal behaviour. *International Journal of Nonferrous Metallurgy,* **2013**, *2*(4), 128-135. http://dx.doi.org/10.4236/ijnm.2013.24019

[13] Brandaleze, E.; Valentini, M.; Santini, L.; Benavidez, E. Study on fluoride evaporation from casting powders. *J. Therm. Anal. Calorim.,* **2018**, *133*(1), 271-277. http://dx.doi.org/10.1007/s10973-018-7227-6

[14] Fan, X.; Deng, Q.; Gan, M.; Chen, X. Roasting oxidation behaviors of ReS_2 and MoS_2 in powdery rhenium-bearing, low-grade molybdenum concentrate. *Trans. Nonferrous Met. Soc. China,* **2019**, *29*(4), 840-848. http://dx.doi.org/10.1016/S1003-6326(19)64994-0

[15] Cui, L.; Lou, F.; Li, Y.; Hou, J.; He, J.L.; Jia, Z.T.; Liu, J-Q.; Zhang, B-T.; Yang, K-J.; Wang, Z-W.; Tao, X-T. Graphene oxide mode-locked Yb:GAGG bulk laser operating in the femtosecond regime. *Opt. Mater.,* **2015**, *42*, 309-312. http://dx.doi.org/10.1016/j.optmat.2015.01.019

[16] Cheema, H.A.; Ilyas, S.; Masud, S.; Muhsan, M.A.; Mahmood, I.; Lee, J. Selective recovery of rhenium from molybdenite flue-dust leach liquor using solvent extraction with TBP. *Separ. Purif. Tech.,* **2018**, *191*, 116-121. http://dx.doi.org/10.1016/j.seppur.2017.09.021

[17] Li, G.; You, Z.; Sun, H.; Sun, R.; Peng, Z.; Zhang, Y.; Jiang, T. Separation of rhenium from lead-rich molybdenite concentrate *via* hydrochloric acid leaching followed by oxidative roasting. *Metals,* **2016**, *6*(11), 282. http://dx.doi.org/10.3390/met6110282

[18] Zhang, B.; Liu, H.Z.; Wang, W.; Gao, Z.G.; Cao, Y.H. Recovery of rhenium from copper leach solutions using ion exchange with weak base resins. *Hydrometallurgy,* **2017**, *173*, 50-56. http://dx.doi.org/10.1016/j.hydromet.2017.08.002

[19] Sun, H.; Li, G.; Bu, Q.; Fu, Z.; Liu, H.; Zhang, X.; Luo, J.; Rao, M.; Jiang, T. Features and mechanisms of self-sintering of molybdenite during oxidative roasting. *Trans. Nonferrous Met. Soc. China,* **2022**, *32*(1), 307-318. http://dx.doi.org/10.1016/S1003-6326(22)65796-0

[20] Shen, L.; Tesfaye, F.; Li, X.; Lindberg, D.; Taskinen, P. Review of rhenium extraction and recycling technologies from primary and secondary resources. *Miner. Eng.,* **2021**, *161*, 106719. http://dx.doi.org/10.1016/j.mineng.2020.106719

[21] Liu, B.; Zhang, B.; Han, G.; Wang, M.; Huang, Y.; Su, S.; Xue, Y.; Wang, Y. Clean separation and purification for strategic metals of molybdenum and rhenium from minerals and waste alloy scraps–A review. *Resour. Conserv. Recycling,* **2022**, *181*, 106232. http://dx.doi.org/10.1016/j.resconrec.2022.106232

[22] Kesieme, U.; Chrysanthou, A.; Catulli, M.; Materials, H. Assessment of supply interruption of rhenium, recycling, processing sources and technologies. *Int. J. Refract. Hard Met.,* **2019**, *82*, 150-158. http://dx.doi.org/10.1016/j.ijrmhm.2019.04.006

[23] Juneja, J.M.; Singh, S.; Bose, D.K. Investigations on the extraction of molybdenum and rhenium values from low grade molybdenite concentrate. *Hydrometallurgy,* **1996**, *41*(2-3), 201-209. http://dx.doi.org/10.1016/0304-386X(95)00056-M

[24] Xiao, C.; Zeng, L.; Xiao, L.; Zhang, G. Thermodynamic analysis of Mo(VI)-Fe(III)-S(VI)-H_2O system for separation of molybdenum and iron. *Metallurgical Research & Technology,* **2018**, *115*(1), 106. http://dx.doi.org/10.1051/metal/2017069

[25] Azadi, M.; Northey, S.A.; Ali, S.H.; Edraki, M. Transparency on greenhouse gas emissions from mining to enable climate change mitigation. *Nat. Geosci.,* **2020**, *13*(2), 100-104. http://dx.doi.org/10.1038/s41561-020-0531-3

[26] Lessard, J.D.; Gribbin, D.G.; Shekhter, L.N.; Materials, H. Recovery of rhenium from molybdenum and copper concentrates during the Looping Sulfide Oxidation process. *Int. J. Refract. Hard Met.,* **2014**, *44*, 1-6. http://dx.doi.org/10.1016/j.ijrmhm.2014.01.003

[27] Sheybani, K.; Javadpour, S.; Materials, H. Mechano-thermal reduction of molybdenite (MoS2) in the presence of Sulfur scavenger: New method for production of molybdenum carbide. *Int. J. Refract. Hard Met.,* **2020**, *92*, 105277. http://dx.doi.org/10.1016/j.ijrmhm.2020.105277

[28] Rafiei, R.; Javadpour, S.; Shariat, M.H.; Ostovari Moghaddam, A.; Materials, H. Effect of processing parameters on the microwave assisted aluminothermic reduction of molybdenite. *Int. J. Refract. Hard Met.,* **2022**, *109*, 105984. http://dx.doi.org/10.1016/j.ijrmhm.2022.105984

[29] Joo, S.H.; Kim, Y.U.; Kang, J.G.; Kumar, J.R.; Yoon, H.S.; Parhi, P.K.; Shin, S.M. Recovery of rhenium and molybdenum from molybdenite roasting dust leaching solution by ion exchange resins. *Mater. Trans.,* **2012**, *53*(11), 2034-2037. http://dx.doi.org/10.2320/matertrans.M2012208

[30] Koleini, S.J.; Barani, K. *Microwave heating applications in mineral processing,* 1st; InTec: Croatia, **2012**.

[31] Kingman, S.W. Recent developments in microwave processing of minerals. *Int. Mater. Rev.,* **2006**, *51*(1), 1-12. http://dx.doi.org/10.1179/174328006X79472

[32] Vorster, W. *The effect of microwave radiation on mineral processing*; PhD dissertation. University of Birmingham, **2001**.

[33] Gerasimov, A.M.; Eremina, O.V. Application microwave radiation for directional changes of layered silicates properties. *Eurasian Mining,* **2021**, (1), 55-60. http://dx.doi.org/10.17580/em.2021.01.11

[34] Chen, T.T.; Dutrizac, J.E.; Haque, K.E.; Wyslouzil, W.; Kashyap, S. The relative transparency of minerals to microwave radiation. *Can. Metall. Q.,* **1984**, *23*(3), 349-351. http://dx.doi.org/10.1179/cmq.1984.23.3.349

[35] Huang, J.; Xu, G.; Liang, Y.; Hu, G.; Chang, P. Improving coal permeability using microwave heating technology—A review. *Fuel,* **2020**, *266*, 117022. http://dx.doi.org/10.1016/j.fuel.2020.117022

[36] Mushtaq, F.; Mat, R.; Ani, F.N. Fuel production from microwave assisted pyrolysis of coal with carbon surfaces. *Energy Convers. Manage.,* **2016**, *110*, 142-153. http://dx.doi.org/10.1016/j.enconman.2015.12.008

[37] Yang, P.; Shan, P.; xu, H.; Chen, J.; Li, Z.; Sun, H. Experimental study on mechanical damage characteristics of water-bearing tar-rich coal under microwave radiation. *Geomech. Geophys.,* **2023**, *10*(1), 3. http://dx.doi.org/10.21203/rs.3.rs-3063964/v1

[38] Lu, G.; Zhou, J.; Li, Y.; Zhang, X.; Gao, W. The influence of minerals on the mechanism of microwave-induced fracturing of rocks. *J. Appl. Geophys.,* **2020**, *180*, 104123. http://dx.doi.org/10.1016/j.jappgeo.2020.104123

[39] Bhattacharya, M.; Basak, T. A review on the susceptor assisted microwave processing of materials. *Energy,* **2016**, *97*, 306-338. http://dx.doi.org/10.1016/j.energy.2015.11.034

[40] Marland, S.; Merchant, A.; Rowson, N. Dielectric properties of coal. *Fuel,* **2001**, *80*(13), 1839-1849. http://dx.doi.org/10.1016/S0016-2361(01)00050-3

[41] Cui, G.; Chen, T.; Feng, X.; Chen, Z.; Elsworth, D.; Yu, H.; Zheng, X.; Pan, Z. Coupled multiscale-modeling of microwave-heating-induced fracturing in shales. *Int. J. Rock Mech. Min. Sci.,* **2020**, *136*, 104520. http://dx.doi.org/10.1016/j.ijrmms.2020.104520

[42] Peng, Z.; Hwang, J.Y. Microwave-assisted metallurgy. *Int. Mater. Rev.,* **2015**, *60*(1), 30-63. http://dx.doi.org/10.1179/1743280414Y.0000000042

[43] Kitchen, H.J.; Vallance, S.R.; Kennedy, J.L.; Tapia-Ruiz, N.; Carassiti, L.; Harrison, A.; Whittaker, A.G.; Drysdale, T.D.; Kingman, S.W.; Gregory, D.H. Modern microwave methods in solid-state inorganic materials chemistry: from fundamentals to manufacturing. *Chem. Rev.,* **2014**, *114*(2), 1170-1206. http://dx.doi.org/10.1021/cr4002353 PMID: 24261861

[44] Ali, A.Y.; Bradshaw, S.M. Confined particle bed breakage of microwave treated and untreated ores. *Miner. Eng.,* **2011**, *24*(14), 1625-1630. http://dx.doi.org/10.1016/j.mineng.2011.08.020

[45] Toifl, M.; Hartlieb, P.; Meisels, R.; Antretter, T.; Kuchar, F. Numerical study of the influence of irradiation parameters on the microwave-induced stresses in granite. *Miner. Eng.,* **2017**, *103-104*, 78-92. http://dx.doi.org/10.1016/j.mineng.2016.09.011

[46] Kingman, S.W.; Jackson, K.; Bradshaw, S.M.; Rowson, N.A.; Greenwood, R. An investigation into the influence of microwave

treatment on mineral ore comminution. *Powder Technol.,* **2004**, *146*(3), 176-184. http://dx.doi.org/10.1016/j.powtec.2004.08.006

[47] Monti, T.; Tselev, A.; Udoudo, O.; Ivanov, I.N.; Dodds, C.; Kingman, S.W. High-resolution dielectric characterization of minerals: A step towards understanding the basic interactions between microwaves and rocks. *Int. J. Miner. Process.,* **2016**, *151*, 8-21. http://dx.doi.org/10.1016/j.minpro.2016.04.003

[48] Chen, G.; Li, L.; Tao, C.; Liu, Z.; Chen, N.; Peng, J. Effects of microwave heating on microstructures and structure properties of the manganese ore. *J. Alloys Compd.,* **2016**, *657*, 515-518. http://dx.doi.org/10.1016/j.jallcom.2015.10.147

[49] Lu, G.M.; Feng, X.T.; Li, Y.H.; Hassani, F.; Zhang, X.; Engineering, R. Experimental investigation on the effects of microwave treatment on basalt heating, mechanical strength, and fragmentation. *Rock Mech. Rock Eng.,* **2019**, *52*(8), 2535-2549. http://dx.doi.org/10.1007/s00603-019-1743-y

[50] Zheng, Y.; Ma, Z.; Zhao, X.; He, L.; Engineering, R. Experimental investigation on the thermal, mechanical and cracking behaviours of three igneous rocks under microwave treatment. *Rock Mech. Rock Eng.,* **2020**, *53*(8), 3657-3671. http://dx.doi.org/10.1007/s00603-020-02135-x

[51] Li, Q.; Li, X.; Yin, T. Effect of microwave heating on fracture behavior of granite: An experimental investigation. *Eng. Fract. Mech.,* **2021**, *250*, 107758. http://dx.doi.org/10.1016/j.engfracmech.2021.107758

[52] Adewuyi, S.O.; Ahmed, H.A.M.; Ahmed, H.M.A. Methods of ore pretreatment for comminution energy reduction. *Minerals,* **2020**, *10*(5), 423. http://dx.doi.org/10.3390/min10050423

[53] 刘纯鹏, 徐有生, 英文版 华J材.. Application of microwave radiation to extractive metallurgy. *JMST,* **1990**, (2), 121-124.

[54] Gholami, H.; Rezai, B.; Mehdilo, ; Hassanzadeh, A.; Yarahmadi, M. Effect of microwave system location on floatability of chalcopyrite and pyrite in a copper ore processing circuit. *Physicochem. Probl. Miner. Proces.,* **2020**, *56*(3), 432-448. http://dx.doi.org/10.37190/ppmp/118799

[55] Brandaleze, E.; Bazán, V.; Orozco, I.; Valentini, M.; Gomez, G. Application of thermal analysis to the rhenium recovery process from copper and molybdenum sulphides minerals. *J. Therm. Anal. Calorim.,* **2018**, *133*(1), 435-441. http://dx.doi.org/10.1007/s10973-018-7104-3

[56] Bale, C.W.; Chartrand, P.; Degterov, S.A.; Eriksson, G.; Hack, K.; Ben Mahfoud, R.; Melançon, J.; Pelton, A.D.; Petersen, S. FactSage thermochemical software and databases. *Calphad,* **2002**, *26*(2), 189-228. http://dx.doi.org/10.1016/S0364-5916(02)00035-4

[57] Cabri, L.J. New data on phase relations in the Cu-Fe-S system. *Econ. Geol.,* **1973**, *68*(4), 443-454. http://dx.doi.org/10.2113/gsecongeo.68.4.443

[58] Aydinyan, S.; Kirakosyan, H.; Niazyan, O.; Kharatyan, S. DTA/TGA study of copper molybdate carbothermal reduction. *Chem. J. Armenia,* **2015**, *68*(2), 196-206.

[59] Haber, J.; Machej, T.; Ungier, L.; Ziółkowski, J. ESCA studies of copper oxides and copper molybdates. *J. Solid State Chem.,* **1978**, *25*(3), 207-218. http://dx.doi.org/10.1016/0022-4596(78)90105-6

[60] Wang, L.Y.; Dong, J.L.; Cai, J.J. Study on mechanism of molybdenum concentrate roasting. *Adv. Mat. Res.,* **2012**, *455-456*, 60-64. http://dx.doi.org/10.4028/www.scientific.net/AMR.455-456.60

[61] Kar, B.B. Carbothermic reduction of hydro-refining spent catalyst to extract molybdenum. *Int. J. Miner. Process.,* **2005**, *75*(3-4), 249-253. http://dx.doi.org/10.1016/j.minpro.2004.08.018

[62] Horikoshi, S.; Serpone, N. Role of microwaves in heterogeneous catalytic systems. *Catal. Sci. Technol.,* **2014**, *4*(5), 1197-1210. http://dx.doi.org/10.1039/c3cy00753g

[63] Drábek, M.; Stein, H. Molybdenite Re-Os dating of Mo-Th-Nb-REE rich marbles: pre-Variscan processes in Moldanubian Variegated Group (Czech Republic). *Geol. Carpath.,* **2015**, *66*(3), 173-179. http://dx.doi.org/10.1515/geoca-2015-0018

[64] Zhang, M.; Liu, C.; Zhu, X.; Xiong, H.; Zhang, L.; Gao, J.; Liu, M. Preparation of ammonium molybdate by oxidation roasting of molybdenum concentrate: A comparison of microwave roasting and conventional roasting. *Chem. Eng. Process.,* **2021**, *167*, 108550. http://dx.doi.org/10.1016/j.cep.2021.108550

[65] Chen, J.; Tang, D.; Zhong, S.; Zhong, W.; Li, B. The influence of micro-cracks on copper extraction by bioleaching. *Hydrometallurgy,* **2020**, *191*, 105243. http://dx.doi.org/10.1016/j.hydromet.2019.105243

[66] Charikinya, E.; Bradshaw, S.M. An experimental study of the effect of microwave treatment on long term bioleaching of coarse, massive zinc sulphide ore particles. *Hydrometallurgy,* **2017**, *173*, 106-114. http://dx.doi.org/10.1016/j.hydromet.2017.08.001

[67] Li, H.; Shi, S.; Lu, J.; Ye, Q.; Lu, Y.; Zhu, X. Pore structure and multifractal analysis of coal subjected to microwave heating. *Powder Technol.,* **2019**, *346*, 97-108. http://dx.doi.org/10.1016/j.powtec.2019.02.009

[68] Yang, K.; Li, S.; Zhang, L.; Peng, J.; Chen, W.; Xie, F.; Ma, A. Microwave roasting and leaching of an oxide-sulphide zinc ore. *Hydrometallurgy,* **2016**, *166*, 243-251. http://dx.doi.org/10.1016/j.hydromet.2016.07.012

[69] Walkiewicz, J.; Kazonich, G.; McGill, S. processing m. Microwave heating characteristics of selected minerals and compounds. *Min. Metall. Explor.,* **1988**, *5*, 39-42. http://dx.doi.org/10.1007/BF03449501

[70] Lovás, M.; Znamenáčková, I.; Zubrik, A.; Kováčová, M.; Dolinská, S. The application of microwave energy in mineral processing–a review. *Acta Montan. Slovaca,* **2011**, *16*(2), 137.